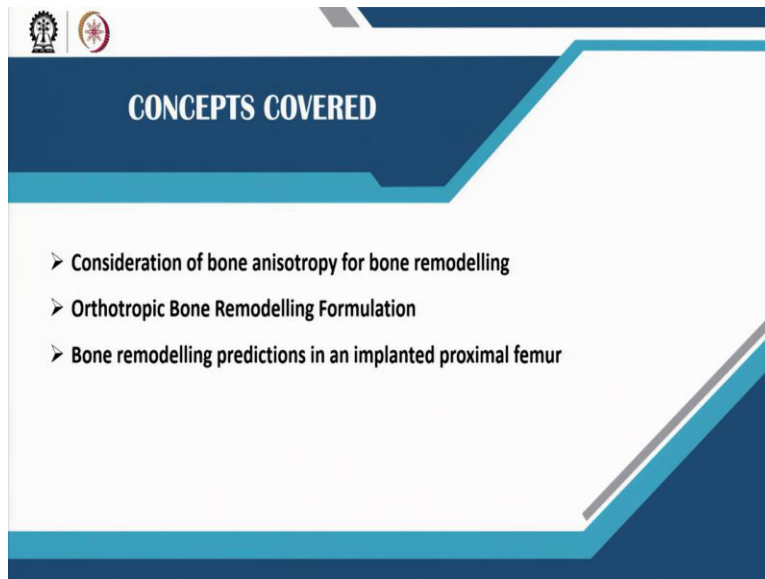


**Biomechanics of Joints and Orthopaedic Implants**  
**Professor. Sanjay Gupta**  
**Department of Mechanical Engineering**  
**Indian Institute of Technology, Kharagpur**  
**Lecture 37**  
**Orthotropic Bone Remodelling**

Good afternoon everybody. Welcome to the lecture 4 of module 7 on orthotropic bone remodeling.

(Refer Slide Time: 0:41)





In this lecture, we will be discussing about consideration of bone anisotropy in bone remodeling. We will be discussing in detail about orthotropic bone remodeling formulation. And thereafter, we will be discussing about bone remodeling predictions in an implanted proximal femur.

(Refer Slide Time: 1:03)

### Consideration of Bone Anisotropy In Bone Remodelling

- Bone exhibits anisotropic material behavior. ✓
- Anisotropic nature of bone could be observed in the trabecular orientation in proximal femur. The trabeculae is arranged in tensile and compressive groups, in order to maintain structural strength of bone.
- Studies of Julius Wolff suggested that the trabecular orientation may coincide with the direction of principal stresses (Wolff, 1986).
- Mechanically driven bone adaptation, leads to changes in bone apparent density and trabecular reorientation (Jacobs et al., 1997).

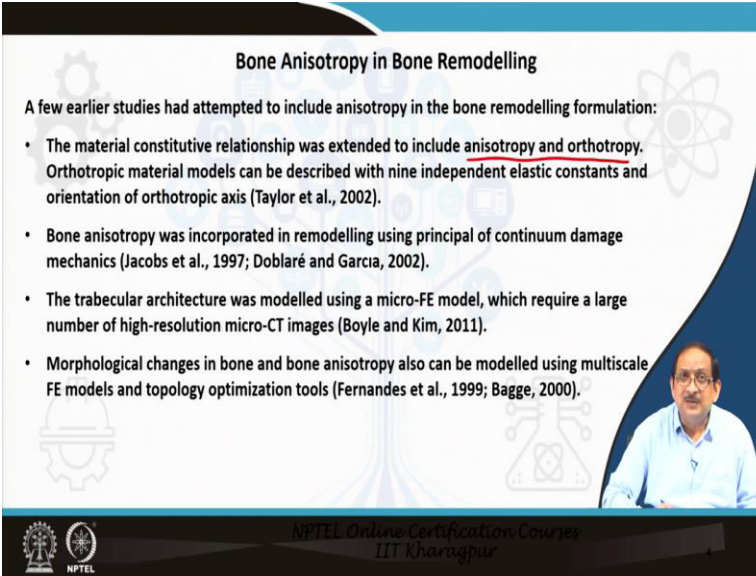


NPTEL Online Certification Courses  
IIT Kharagpur

Now, bone, as you know, exhibits anisotropic material behavior. We have discussed this issue earlier in module 5 quite in detail. Now, anisotropic nature of bone could be observed in the trabecular orientation in a proximal femur as presented in the figure on the right. The trabeculae is arranged in tensile and compressive groups in order to maintain structural strength of bone.

Now, studies of Julius Wolff suggested that the trabecular orientation may coincide with the direction of principal stresses. Mechanically driven bone adaptation leads to changes in bone apparent density and trabecular orientation.

(Refer Slide Time: 2:17)



**Bone Anisotropy in Bone Remodelling**

A few earlier studies had attempted to include anisotropy in the bone remodelling formulation:

- The material constitutive relationship was extended to include anisotropy and orthotropy. Orthotropic material models can be described with nine independent elastic constants and orientation of orthotropic axis (Taylor et al., 2002).
- Bone anisotropy was incorporated in remodelling using principle of continuum damage mechanics (Jacobs et al., 1997; Doblaré and Garcia, 2002).
- The trabecular architecture was modelled using a micro-FE model, which require a large number of high-resolution micro-CT images (Boyle and Kim, 2011).
- Morphological changes in bone and bone anisotropy also can be modelled using multiscale FE models and topology optimization tools (Fernandes et al., 1999; Bagge, 2000).

NPTEL Online Certification Courses  
IIT Kharagpur

Let us first discuss about few previous studies that attempted to include bone anisotropy in the bone remodelling formulation. Now, the material constitutive relationship was extended to include anisotropy and orthotropy. Orthotropic material models can be described with 9 independent elastic constants and orientation of the orthotropic axis. Bone anisotropy was incorporated in remodelling using principle of continuum damage mechanics.

The trabecular architecture was modelled using a micro FE model, which requires a large number of high-resolution micro CT scan images. Morphological changes in bone and bone anisotropy also can be modeled using multi-scale FE models and topology optimization tools.

(Refer Slide Time: 3:28)

**Orthotropic Bone Remodelling Formulation**

- The orthotropic algorithm comprised of two sequential operations:
  - ✓ (1) Estimation of element orientation
  - ✓ (2) Modification of elastic moduli along orthogonal directions
- At every iteration, FE models were solved and the stress,  $\sigma_{ij}$ , and strain,  $\epsilon_{ij}$ , tensors were calculated for each element.
- Eigen analysis of the guiding stress tensor gives the element principal stress directions,  $\sigma_{pv}$  and the principal stress values,  $\sigma_p$

$$\sigma_{pv}^g, \sigma_p^g = \begin{bmatrix} \sigma_{pv}^{min} & \sigma_{pv}^{med} & \sigma_{pv}^{max} \\ \sigma_{pv}^{min} & \sigma_{pv}^{med} & \sigma_{pv}^{max} \\ \sigma_{pv}^{min} & \sigma_{pv}^{med} & \sigma_{pv}^{max} \end{bmatrix}, \begin{bmatrix} \sigma_p^{min} & 0 & 0 \\ 0 & \sigma_p^{med} & 0 \\ 0 & 0 & \sigma_p^{max} \end{bmatrix}$$

NPTEL Online Certification Courses  
IIT Kharagpur

We would like to present an orthotropic bone remodeling formulation that we just proposed recently. The main steps involved in the remodeling process are presented here. So, the orthotropic formulation is comprised of two sequential operations. One was the estimation of element orientation. The other operation was the modification of elastic moduli along orthogonal directions. Now, let us present the details in a sequential manner.

At every iteration, FE models were solved and the stresses that is  $\sigma_{ij}$  and the strain  $\epsilon_{ij}$ , the tensors were calculated for each element. Now, Eigen analysis of the guiding stress tensor gives the element principal directions  $\sigma_{pv}$  and the principal stress values  $\sigma_p$  as indicated here in the slide.

(Refer Slide Time: 5:06)

**Orthotropic Bone Remodelling Formulation**

The strain stimulus along the target directions were then computed for each element from  $\sigma_{pv}^g$  and  $\epsilon_{ij}^{max}$ , using the equation:

$$\epsilon_{ij}^* = \sigma_{pv}^{gT} \epsilon_{ij}^{max} \sigma_{pv}^g$$

where,  $\epsilon_{ij}^{max}$  is known as the strain envelope. It is the maximum absolute strain components considering all the loads cases, as shown in following expression:

$$\epsilon_{ij}^{max} = \max(\text{abs}(\epsilon_{ij}^{n=1}, \epsilon_{ij}^{n=2}, \epsilon_{ij}^{n=3}, \dots, \epsilon_{ij}^{max})), \quad 1 \leq n \leq n_{max}$$

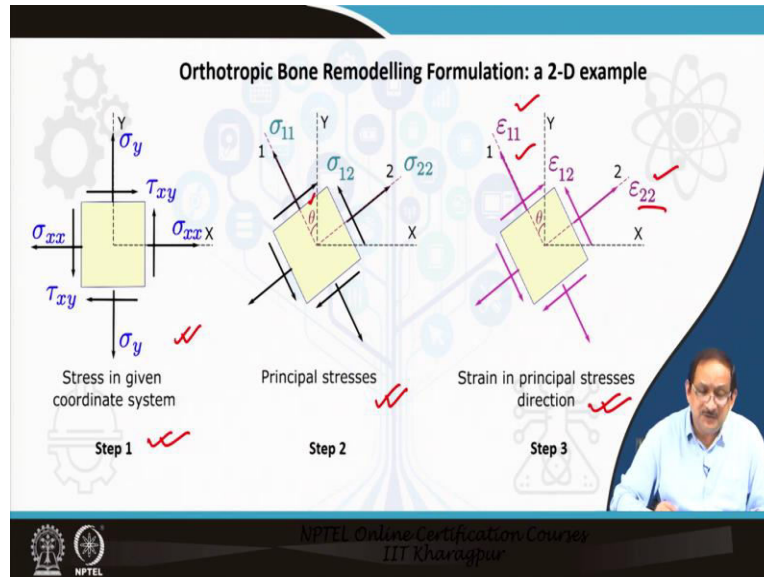
Orthotropic bone remodelling progresses assuming,  $\epsilon_{ij}^*$  as the mechanical stimulus, along three orthogonal axes. The material properties and the orthotropic orientation of each element were updated based on  $\epsilon_{ij}^*$ .

NPTEL Online Certification Course  
IIT Kharagpur

The strain stimulus along the target directions was then computed for each element from the stress tensor and the strain or the maximum strain tensor using the equation as indicated here. So, it is a matter of transformation of the  $\epsilon_{ij}^{max}$ , known as the strain envelope. So, it is the maximum absolute strain components considering all the load cases as shown in the following expression.

Now, if multiple loads cases are used, epsilon max can be determined. Orthotropic bone remodeling progresses, assuming the  $\epsilon_{ij}^*$  as the mechanical stimulus. This is a very important aspect of the formulation. So, it assumes  $\epsilon_{ij}^*$ , the strain, as the mechanical stimulus along three orthogonal axis. The material properties and the orthotropic orientation of each element were updated based on  $\epsilon_{ij}^*$ .

(Refer Slide Time: 6:58)



Now, let us try to give you a diagrammatic representation of the procedure of transforming the strain along the principal stress directions. The image shown here shows the overview of the strain stimulus calculation considering a 2D case. So, we consider a 2D case for simplicity of understanding. Each element, as you can see in step 1, each element will have a stress tensor associated with it.

The principal stress directions can be calculated in step 2 using Eigen analysis, as you can see, the theta can be determined in case of a 2D problem. In 3D case, three angles actually need to be defined to define the orientation of the principal stress. Now, the strain tensor is transformed along the principal stress direction as indicated here in the figure in order to estimate the mechanical stimulus which is now strain along 3 orthogonal directions.

Since, it is a 2D problem, we have  $\epsilon_{11}$  and  $\epsilon_{22}$  as indicated here in the figure. The material properties are modified based on the values of these strains.

(Refer Slide Time: 9:09)

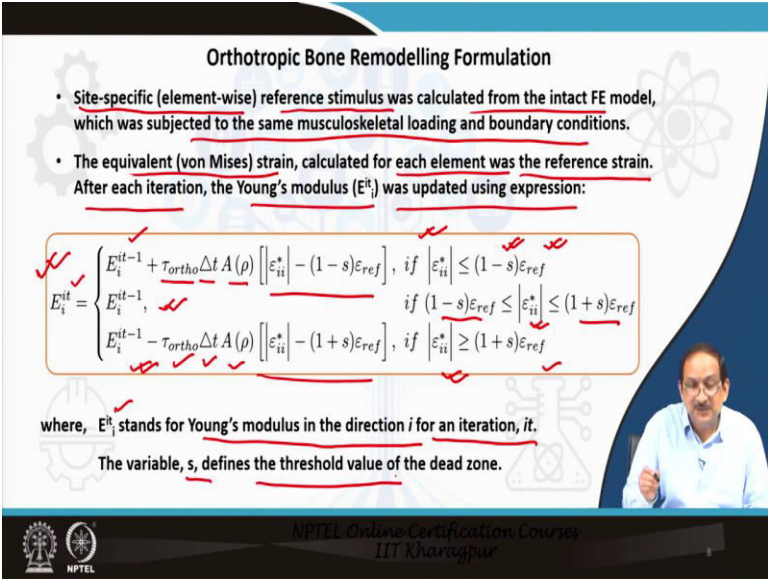
**Orthotropic Bone Remodelling Formulation**

- Site-specific (element-wise) reference stimulus was calculated from the intact FE model, which was subjected to the same musculoskeletal loading and boundary conditions.
- The equivalent (von Mises) strain, calculated for each element was the reference strain. After each iteration, the Young's modulus ( $E_i^*$ ) was updated using expression:

$$E_i^{it} = \begin{cases} E_i^{it-1} + \tau_{ortho} \Delta t A(\rho) \left[ \left| \varepsilon_{ii}^* \right| - (1-s)\varepsilon_{ref} \right], & \text{if } \left| \varepsilon_{ii}^* \right| \leq (1-s)\varepsilon_{ref} \\ E_i^{it-1}, & \text{if } (1-s)\varepsilon_{ref} \leq \left| \varepsilon_{ii}^* \right| \leq (1+s)\varepsilon_{ref} \\ E_i^{it-1} - \tau_{ortho} \Delta t A(\rho) \left[ \left| \varepsilon_{ii}^* \right| - (1+s)\varepsilon_{ref} \right], & \text{if } \left| \varepsilon_{ii}^* \right| \geq (1+s)\varepsilon_{ref} \end{cases}$$

where,  $E_i^*$  stands for Young's modulus in the direction  $i$  for an iteration,  $it$ .

The variable,  $s$ , defines the threshold value of the dead zone.



Now, orthotropic bone remodeling formulation is done based on a site-specific or elements-specific approach. So, site-specific or elements specific reference stimulus was calculated from the intact FE model which was subject to the same musculoskeletal loading and boundary conditions. So, similar to the procedure of any other remodeling formulation, we need to have an intact FE model and the implanted FE model.

So, the reference stimulus is calculated from the intact FE model. The equivalent Von Mises or equivalent strain calculated for each element was the reference strain. At each iteration, the Young's modulus  $E_i$  was updated using the following expression as indicated in the slide. The change in Young's modulus was proportional to the change in remodelling signal in the case of an implanted bone model.

And the reference stimulus corresponding to the intact bond model. Now, in the equations that are presented here, the whole formulation is quite similar to the isotropic formulation based on the strain energy density or strain energy per unit of bone mass. So, here we see that the previous E modulus  $E_i$  corresponding to  $it-1$  is updated to  $E_{it}$  when we add the terms concerning the difference in the mechanical stimulus.

And of course the adaptation rate, the time step, and the free surface area of the bone volume. Now, this first relationship corresponds to the condition when the strain is less than a certain reference value and beyond the range of the dead zone as defined here. Now, if the strain value is

located within the limits of the dead zone, no remodeling takes place. If the strain value is greater than the reference stimulus and in the limits of the dead zone, then we have another equation given by the difference in the mechanical stimulus as well as the adaptation rate, the time step, and the free surface area of the bone.

These are the main governing equations of the orthotropic boundary modeling formulation. Now, here  $E_{it}$  stands for the Young's modulus in the direction  $i$  corresponding to the iteration  $it$  and the variable  $s$  is defined as the threshold value of the dead zone.

(Refer Slide Time: 13:26)

**Orthotropic Bone Remodelling Formulation**

- The simulation time step was calculated in each iteration using the expression,
 
$$\tau_{ortho}\Delta t = \frac{\Delta E_{max}}{\left\{ A(\rho) \left[ \epsilon_{ii}^* - (1 \pm s)\epsilon_{ref} \right] \right\}_{max}}$$
- where,  $A(\rho) = a(\rho) V$ . The constant  $\Delta E_{max}$  was calculated for a maximum change in density of  $0.865 \text{ g.cm}^{-3}$ .
- The free surface area per unit volume  $a(\rho)$ , was represented as a function of the apparent density ( $\rho$  in  $\text{g.cm}^{-3}$ ) using the following expression.
 
$$a(\rho) = -0.0293 + 8.5124\rho - 4.8870\rho^2 + 1.5680\rho^3 + 3.7182\rho^4 - 1.6352\rho^5$$

The graph on the right shows the Remodelling rate on the y-axis and Stimulus on the x-axis. The y-axis is divided into 'Apposition (gain)' (positive) and 'Resorption (loss)' (negative). The x-axis has a 'Dead Zone' between  $(1-s)\epsilon_{ref}$  and  $(1+s)\epsilon_{ref}$ . A stimulus  $\epsilon_{ii}^*$  is shown above the dead zone, and a reference stimulus  $\epsilon_{ref}$  is shown below it. The area under the curve is shaded green for apposition and red for resorption.

NPTEL Online Certification Courses  
IIT Kharagpur

Now, similar to the isotropic formulation, the simulation time step was calculated in each iteration using the expression as presented here. Here also  $\tau\Delta t$  is the simulation time step and the  $\Delta E_{max}$ , the constant  $\Delta E_{max}$ , was calculated for a maximum change in density of 0.865. And the  $a(\rho)$  is the free surface area of the cancellous bone.

Now, the free surface area per unit volume or the surface area density as discussed earlier can be represented as a function of apparent density using the following expression. Now, on the right, the whole process can be summarized. Based on the reference stimulus, we can define the dead zone and the remodeling rate whether it is gaining bone density or reduction in bone density given by apposition and bone resorption, respectively can occur based on the formulation explained earlier.



(Refer Slide Time: 15:12)

### Orthotropic Bone Remodelling Formulation

- The representative Young's modulus for a bone element,  $E_{rep}$ , and the shear modulus,  $G_{ij}^{it}$ , were calculated as follows:

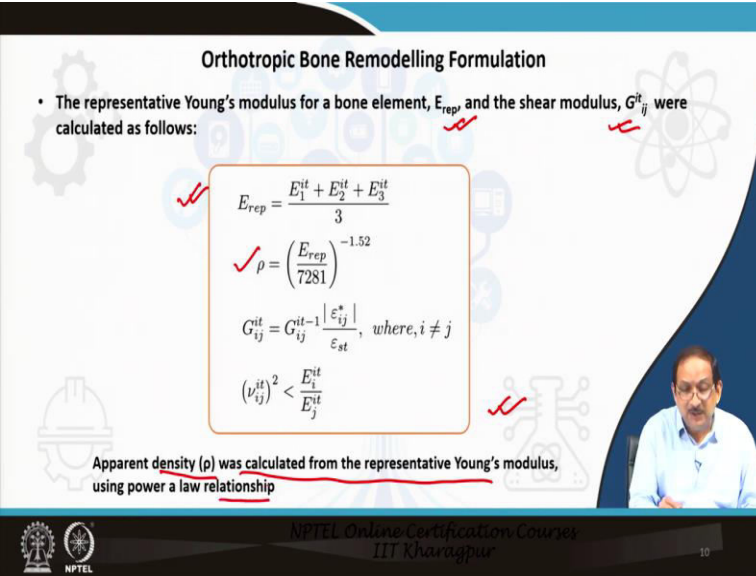
$$E_{rep} = \frac{E_1^{it} + E_2^{it} + E_3^{it}}{3}$$

$$\rho = \left( \frac{E_{rep}}{7281} \right)^{-1.52}$$

$$G_{ij}^{it} = G_{ij}^{it-1} \frac{|\epsilon_{ij}^*|}{\epsilon_{st}}, \text{ where, } i \neq j$$

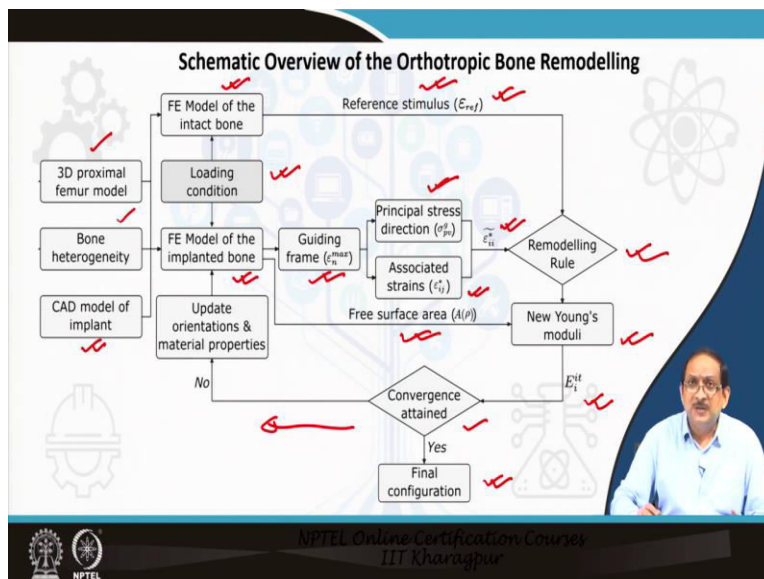
$$(\nu_{ij}^{it})^2 < \frac{E_i^{it}}{E_j^{it}}$$

Apparent density ( $\rho$ ) was calculated from the representative Young's modulus, using power a law relationship



The representative Young's modulus of a bone element  $E$  represents  $E_{rep}$ , and the shear modulus was calculated as indicated in the expressions presented here in the slide. The apparent density  $\rho$  was calculated from the representative Young's modulus using a power law relationship.

(Refer Slide Time: 15:48)



Now, this schematic overview of the orthotropic bone modeling simulation can be presented here in the form of a flowchart. Now, here as you can see that there is a 3D proximal femur model based on the CT scan data; we can actually allocate heterogeneous bone material properties. We

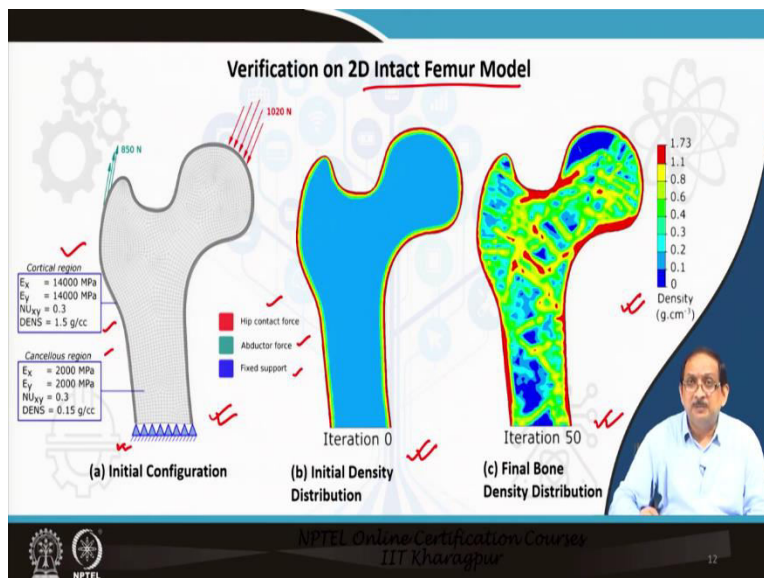
can have the CAD model of the implant, and we can generate an FE model of the intact femur as well as the FE model of the implanted femur.

So, we need both. The same loading conditions need to be applied to these two models separately. So, from the intact bone model, we can actually calculate the reference stimulus  $\epsilon_{ref}$  and we can actually find out the guiding frame or the strain envelope given by  $\epsilon_{max}$ . We need to determine the principal stress directions for an element and the associated strains can be transformed along that direction.

So, we obtain the strain stimulus and we compare it with the reference stimulus. And based on the comparison, we can apply the remodeling rule; the difference of the strain stimulus that is the ref remodeling signal and the reference signal. So, when we apply the remodeling rule, we can obtain the new Young's moduli of the bone elements. And of course, we can use the free surface area of available bone in the calculation of the new Young's moduli.

So, we update Young's modulus value of the bone of a bone element and we keep on iterating until convergence is achieved and the final configuration of the implant-bone model reaches equilibrium of bone remodeling.

(Refer Slide Time: 18:49)

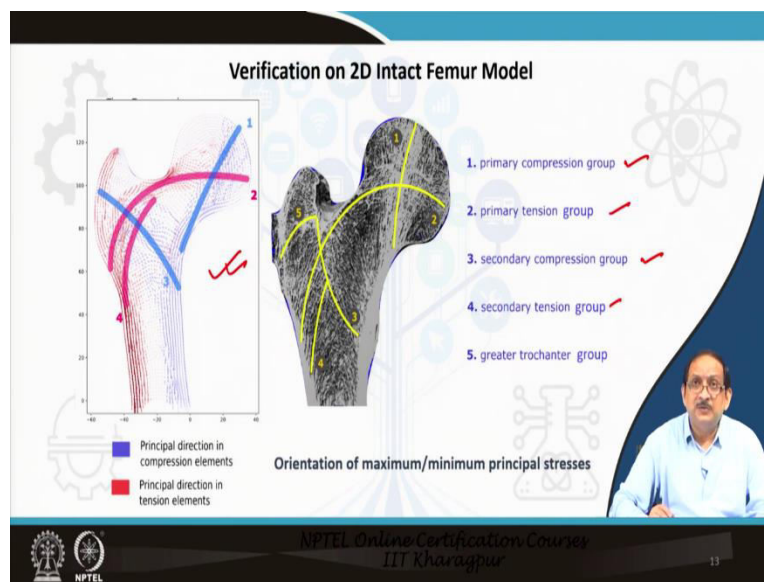


The orthotropic remodeling algorithm was first tested on a 2D model of the intact femur for the purpose of verification. The 2D plane stress model of the proximal femur has cortical as well as cancellous regions. Remember or please note that there are only two regions in the initial

configuration: one cortical region covering the inner cancellous bone region. So, the 2D plane stress model of a proximal femur having cortical and cancellous bone regions actually contained a total number of 3024 elements.

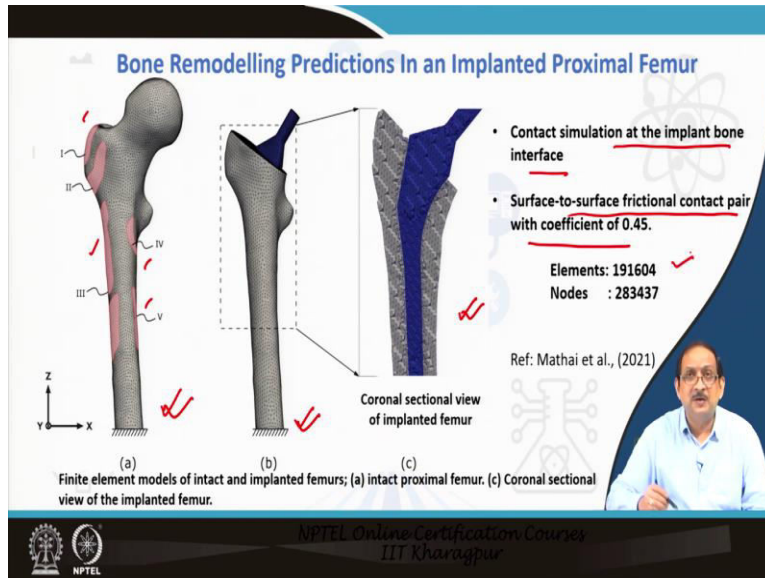
And we actually applied the hip contact force, the abductor muscle force and applied an artificial constraint at one end. Now, figure b shows the initial bone density distribution. The dominant directions, that is the absolute maximum principles stress, were calculated and the material properties were updated proportionally to the strain value. Figure c shows the final bone density distribution after attainment of equilibrium of orthotropic bone remodeling as you can see from the variation in bone density distribution in the 2D plane model.

(Refer Slide Time: 20:47)



Functional trabeculae usually groups within a proximal femur such as primary compressive group, the secondary compressive group, the primary tensile group, and the secondary tensile group were adequately predicted in the 2D model as can be observed in the figure. The figure on the left is the simulation results corresponding to the 2D intact femur model. So, these results confirm the suitability of using the orthotropic remodelling algorithm for further investigations on 3D FE model of the implanted proximal femur.

(Refer Slide Time: 21:46)



So, we come to the third topic of this lecture that is bone remodeling predictions in an implanted proximal femur. So, as discussed earlier, patient-specific 3D models of the intact figure a and implanted proximal femur figure b were developed based on the CT scan data set of a subject. So, the shaded region represents the muscle attachment sites of different muscles such as the gluteus, vastus lateralis, vastus intermedius, vastus medialis, and abductors.

Both the intact and implanted models were meshed with ten noded tetrahedral elements. Now, you can see a coronal sectional view of the implanted femur, which is presented as the figure c here. Now, contact simulation at the implant-bone interface was employed using surface to surface frictional contact pair with friction coefficient equal to 0.45. So, the total number of elements was about 200,000 elements.

(Refer Slide Time: 23:23)

**3D FE Modelling of Intact and Implanted Femur**

- An image processing software, MIMICS (Materialise, Leuven, Belgium) was used for generating 3D surface geometry of the right intact femur based on a CT-scan dataset. A 3D model of the TriLock hip stem (DePuy Orthopaedics, Warsaw, IN) was used for the analysis.

• 10-node tetrahedral elements. ✓

• Each bone element is linearly elastic and isotropic. ✓

• Surface-to-surface frictional contact pair with coefficient of 0.45. ✓

$$\rho = \rho_1 + (\rho_2 - \rho_1) \times \frac{HU - HU_1}{HU_2 - HU_1}$$

$(\rho_1, HU_1) : 0.022 \text{ gm.cm}^{-3}, 0 \text{ HU}$

$(\rho_2, HU_2) : 1.73 \text{ gm.cm}^{-3}, 1700 \text{ HU}$

Young's Modulus of bone element assigned based on:  $E = 7281 \rho^{1.52} \text{ MPa}$  ✓

Young's Modulus of the implant material: 110 GPa (Titanium Alloy) ✓

HU: CT grey value in Hounsfield Units

NPTEL Online Certification Course  
IIT Kharagpur

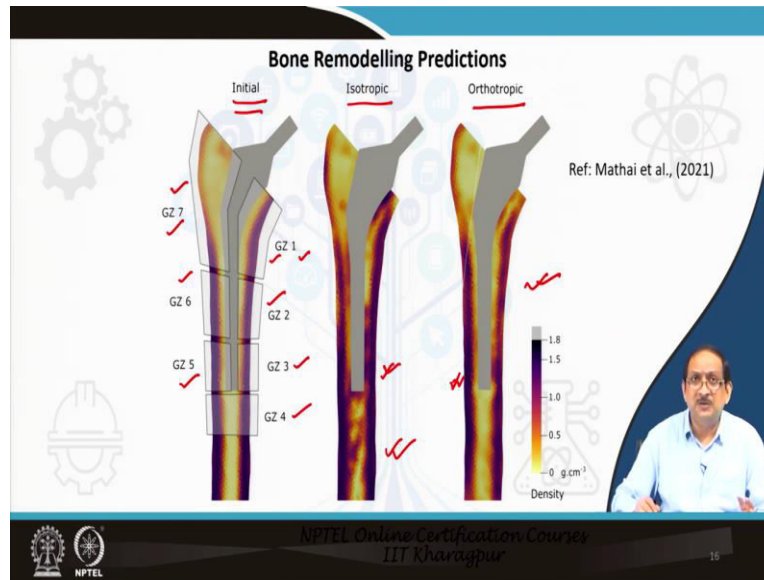
Let me present a summary of the 3D finite element modeling procedure of intact and implanted femur. Now, as discussed earlier, an image processing software was used to generate 3D surface geometry of the right intact femur based on a CT scan data set. Now, a 3D model of the trial of hip stem was considered for the analysis. The FE models were actually meshed with ten noded tetrahedral elements having edge length varying between 0.3 to 0.8 millimeter.

So, both the intact and implanted models were meshed, following this specification. Each bone element was considered to be linearly elastic and isotropic to start with. Surface to surface contact elements having a friction coefficient of 0.45 was used at the implant-bone interface. The bone material properties were extracted from the CT scan data using the linear calibration of apparent density and CT grey value and using the power-law relationship between bone Young's modulus and apparent density.

The Young's modulus of the implant material was taken as 110 GPA corresponding to the titanium alloy. Now, loading configuration included maximum load cases from other common daily activities like sitting up from the chair and sitting down along with peak load cases of normal walking and stair climbing.

Now, peak load instances of hip joint reaction force or hip contact force were considered for these activities.

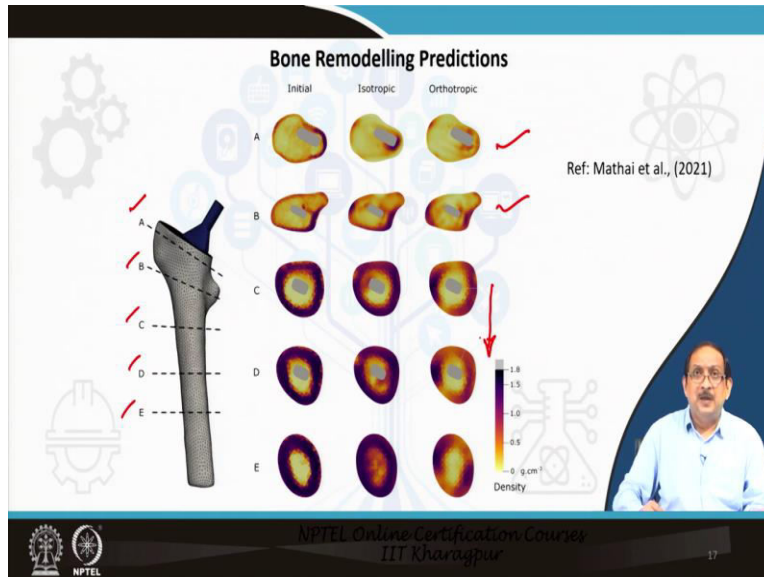
(Refer Slide Time: 25:57)



Now, let us come to the results predicted by the orthotropic bone remodeling simulation and we will compare the results with those predicted by the isotropic bone remodeling predictions that is based on the strain energy per unit of bone mass. So, in this slide, we first present the initial bone density configuration and we have indicated the Gruen zones from 1 to 7.

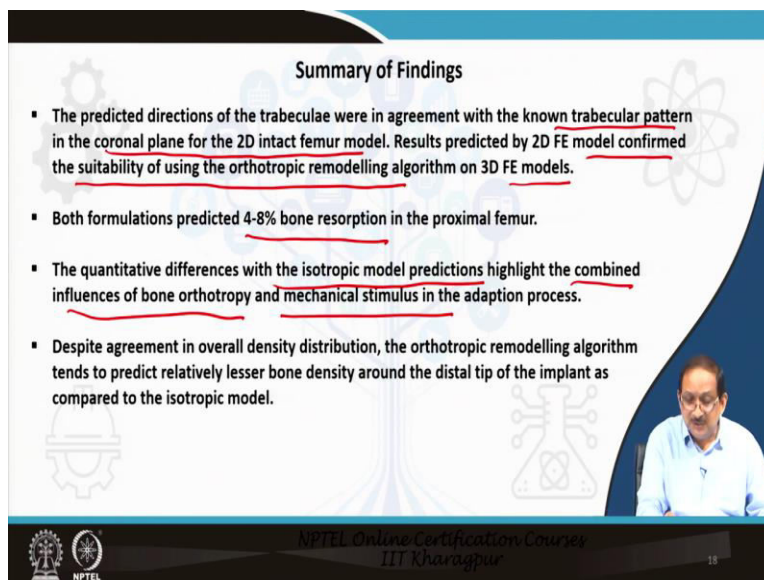
The bone density changes predicted by the two formulations that is the isotropic based and orthotropic based formulation, were generally comparable in the proximal regions in Gruen zones 1, 2, 6, and 7 as indicated in the figure. However, higher quantitative deviations in bone apposition were observed towards the distal end of the implant, mostly around Gruen zone 3, 4, and 5, which is somewhere here, in corresponding to the two formulations. So, the quantitative deviations were mostly concentrated around the distal end of the implant.

(Refer Slide Time: 27:55)



So, we plot the sectional views. As you can see, we have taken five sections from section A, B, C, D, E. We move from the proximal end to the distal end of the implant, and you can see here as well that the bone density distributions were generally comparable in the proximal regions whereas, the deviations started creeping in when we move more towards the distal end of the implant.

(Refer Slide Time: 28:45)

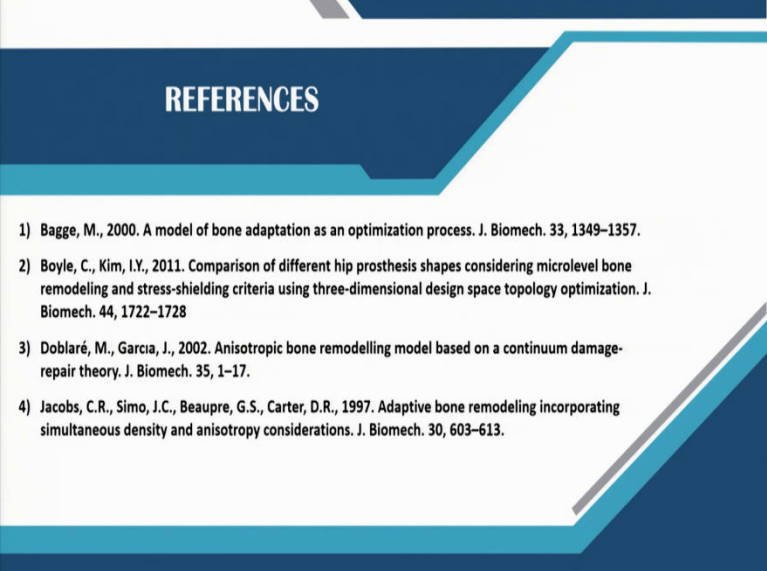


So, let us now present the summary of the findings. The predicted directions of the trabeculae were in agreement with the known trabecular pattern in the coronal plane for the 2D intact femur

model. Results predicted by the 2D FE model confirmed the suitability of using the orthotropic remodeling algorithm on 3D finite element models of the implanted bone structure. Both formulations predicted 4 to 8 percent bone resorption in the proximal femur.

That means both the isotropic as well as the orthotropic bone remodeling formulations predicted about 4 to 8 percent bone resorption in the proximal femur. The quantitative differences with the isotropic model predictions highlight the combined influences of bone orthotropic and the mechanical stimulus in the adaptation process. Despite agreement in overall density distribution, the orthotropic remodeling algorithm tends to predict relatively lesser bone density around the distal tip of the implant as compared to the isotropic model.

(Refer Slide Time: 30:25)



## REFERENCES

- 1) Bagge, M., 2000. A model of bone adaptation as an optimization process. *J. Biomech.* 33, 1349–1357.
- 2) Boyle, C., Kim, I.Y., 2011. Comparison of different hip prosthesis shapes considering microlevel bone remodeling and stress-shielding criteria using three-dimensional design space topology optimization. *J. Biomech.* 44, 1722–1728
- 3) Doblaré, M., Garcia, J., 2002. Anisotropic bone remodelling model based on a continuum damage-repair theory. *J. Biomech.* 35, 1–17.
- 4) Jacobs, C.R., Simo, J.C., Beaupre, G.S., Carter, D.R., 1997. Adaptive bone remodeling incorporating simultaneous density and anisotropy considerations. *J. Biomech.* 30, 603–613.



## REFERENCES

- 5) Fernandes, P., Rodrigues, H., Jacobs, C., 1999b. A model of bone adaptation using a global optimisation criterion based on the trajectorial theory of wolff. *Comput. Methods Biomech. Biomed. Engin.* 2, 125–138.
- 6) Mathai, B., Dhara, S., Gupta, S., 2021. Orthotropic bone remodelling around uncemented femoral implant: a comparison with isotropic formulation. *Biomech. Model. Mechanobiol.* 20, 1115–1134.
- 7) Taylor, W., Roland, E., Ploeg, H., Hertig, D., Klabunde, R., Warner, M., Hobatho, M., Rakotomanana, L., Clift, S., 2002. Determination of orthotropic bone elastic constants using FEA and modal analysis. *J. Biomech.* 35, 767–773.
- 8) Wolff, J., 1986. *The law of bone remodelling*. Translated by P. Maquet and R. Furlong. New York, Springer 1, 8.

The list of references is presented here in two slides based on which the lecture was prepared.  
Thank you for listening.